Spin relaxation in graphene nanoribbons in the presence of substrate surface roughness

Zahra Chaghazardi, Shoeib Babaee Touski, Mahdi Pourfath, and Rahim Faez

Citation: Journal of Applied Physics **120**, 053904 (2016); doi: 10.1063/1.4960354
View online: http://dx.doi.org/10.1063/1.4960354
View Table of Contents: http://scitation.aip.org/content/aip/journal/jap/120/5?ver=pdfcov
Published by the AIP Publishing

Spin relaxation in graphene nanoribbons in the presence of substrate surface roughness

Zahra Chaghazardi,[1] Shoeib Babaee Touski,[2] Mahdi Pourfath,[2,3,4,a)] and Rahim Faez[1]
[1]*Department of Electrical Engineering, Sharif University of Technology, Tehran 11365-8639, Iran*
[2]*School of Electrical and Computer Engineering, University of Tehran, Tehran 14395-515, Iran*
[3]*School of Nano Science, Institute for Research on Fundamental Sciences (IPM), Tehran 19395-5531, Iran*
[4]*Institute for Microelectronics, Technische Universität Wien, Gußhausstraße 27–29/E360, A-1040 Wien, Austria*

(Received 9 May 2016; accepted 22 July 2016; published online 5 August 2016)

In this work, spin transport in corrugated armchair graphene nanoribbons (AGNRs) is studied. We survey combined effects of spin-orbit interaction and surface roughness, employing the non-equilibrium Green's function formalism and multi-orbitals tight-binding model. Rough substrate surfaces have been statistically generated and the hopping parameters are modulated based on the bending and distance of corrugated carbon atoms. The effects of surface roughness parameters, such as roughness amplitude and correlation length, on spin transport in AGNRs are studied. The increase of surface roughness amplitude results in the coupling of σ and π bands in neighboring atoms, leading to larger spin flipping rate and therefore reduction of the spin-polarization, whereas a longer correlation length makes AGNR surface smoother and increases spin-polarization. Moreover, spin diffusion length of carriers is extracted and its dependency on the roughness parameters is investigated. In agreement with experimental data, the spin diffusion length for various substrate ranges between 2 and 340 μm. Our results indicate the importance of surface roughness on spin-transport in graphene. *Published by AIP Publishing*. [http://dx.doi.org/10.1063/1.4960354]

I. INTRODUCTION

Spintronics employs spin degree of freedom in logic and memory devices to improve their efficiency. It decreases electrical power consumption and increases both information processing speed and integration density.[1] Experimentally, spin transport is investigated in many materials such as metals, semiconductors, and carbon based materials. Carbon-based materials however attract tremendous attention due to their low intrinsic spin-orbit and hyperfine coupling.[2]

Graphene—a two-dimensional monolayer of graphite—was realized for the first time in 2004.[3] Owing to its physical extraordinary properties, graphene has attracted growing interest in research from fundamental physics to electronics, spintronics, and thermoelectrics. Importantly, it is an attractive material for electronics and spintronics due to its specific physical properties such as high electron mobility and gate-tunable carrier concentration.[4] Furthermore, achievement of room-temperature spin transport with relatively long spin relaxation time[2,5–7] makes graphene nanoribbons the best candidate for spintronics.[8] Recent experimental studies have already identified the advantages of graphene for spintronics in comparison with metals and semiconductors.[4]

It is supposed that graphene has a relatively small spin-orbit interaction due to low atomic number of carbon $Z = 6$.[2] Various theoretical values are estimated for the gap opening by spin-orbit interaction at the K-point: 1 μeV,[9,10] 24 μeV,[11] 50 μeV,[12] and 200 μeV.[13]

Based on the theoretical perditions, the weak spin-orbit interaction in graphene results in spin relaxation times in the order of microseconds.[8,14] However, much shorter relaxation times in the range of pico- to few nanoseconds have been experimentally reported.[5,7,15,16] The discrepancy between theory and experiment is not yet well understood and the origin of spin relaxation in graphene is under debate.[4] Various sources of spin-relaxation are discussed in Refs. 17 and 18. It has been suggested that extrinsic effects,[19] such as substrate and adatoms,[14,20,21] ripples,[22] and charged impurities,[23,24] are the causes of the spin-relaxation time degradation in graphene.

Substrate surface roughness can affect spin transport in graphene.[25–27] In an ideal graphene, sheet spin-orbit interaction between nearest neighbors vanishes,[2] whereas next nearest neighbors have negligible effects on spin flipping.[13] Substrate surface roughness enhances mixing between σ and π orbitals by hopping between neighboring atoms,[2] and therefore increases spin-orbit interaction. In this context, spin transport has been studied for a curved graphene nanoribbon[28] and also in the presence of random spin-orbit coupling (SOC).[29,30] However, a careful and comprehensive analysis of spin-transport with realistic surface is missing. In this work, spin transport in corrugated graphene nanoribbon is studied, employing an atomistic approach based on the non-equilibrium Green's function (NEGF) formalism.[31]

II. APPROACH

The Hamiltonian can be described as

$$H = H_{\mathrm{TB}} + H_{\mathrm{SO}}, \tag{1}$$

where H_{TB} is the nearest-neighbor tight-binding Hamiltonian excluding spin-orbit coupling

a)pourfath@ut.ac.ir and pourfath@iue.tuwien.ac.at

$$H_{\mathrm{TB}} = \sum_{\langle i,j\rangle;l,m} (\epsilon_{l,m}\delta_{i,j}\delta_{l,m} - t_{i,j;l,m})\hat{c}^{\dagger}_{i,j;l,m}\hat{c}_{i,j;l,m}, \tag{2}$$

where i and j are indices of atoms and $\langle i,j\rangle$ runs over first-nearest neighbors, l and m are the orbital indices, which are $p_{x,y,z}$ and s orbitals, ϵ represents the on-site potential, and t is the hopping parameter. The selected values of discussed parameters can be found in Table I. In Eq. (1), H_{SO} is the spin-orbit coupling term. The spin orbit Hamiltonian can be modeled as inter-atomic or intra-atomic. Inter-atomic model (based on an effective interaction) can be obtained from a multi-orbital intra-atomic model. We employed an intra-atomic Hamiltonian that can be written as[2,28]

$$H_{\mathrm{SO}} = \lambda \hat{L}\cdot\hat{S}, \tag{3}$$

where λ is the spin-orbit coupling (SOC) constant that is chosen to be 12 meV.[32,33] $\hat{L}$ and $\hat{S}$ are angular momentum and spin operators, respectively. Intra-atomic spin-orbit coupling between $p_{x\uparrow}$, $p_{y\uparrow}$, $p_{z\uparrow}$ $p_{x\downarrow}$, $p_{y\downarrow}$, $p_{z\downarrow}$ orbitals is given by

$$H_{\mathrm{SO}} = \frac{\lambda}{2}\begin{pmatrix} 0 & -i & 0 & 0 & 0 & 1 \\ i & 0 & 0 & 0 & 0 & -i \\ 0 & 0 & 0 & -1 & i & 0 \\ 0 & 0 & -1 & 0 & i & 0 \\ 0 & 0 & -i & -i & 0 & 0 \\ 1 & i & 0 & 0 & 0 & 0 \end{pmatrix}. \tag{4}$$

Fig. 1(b) shows intra-atomic spin orbit interaction occurs only within an atom and it is transferred to neighboring atoms through hopping between sigma bonds. Although s orbital does not contribute to spin-orbit matrix, but it affects spin transport through bonding. The effective SOC constant is inversely proportional to $sp\sigma$ hopping parameter in second order.[9]

Substrate surface is an statistical phenomena which can be modeled by a Gaussian auto-correlation function (ACF)[25]

$$R(x,y) = \delta h^2 \exp\left(-\frac{x^2}{{L_x}^2} - \frac{y^2}{{L_y}^2}\right). \tag{5}$$

L_x and L_y are the roughness correlation lengths along the x and y-directions, respectively. The transport direction is assumed to be along the x-axis and the transverse direction is along the y-axis. δh is the root mean square of the height fluctuation. For generating roughness in spatial domain, a random phase should be added to the power spectrum of the auto-correlation function followed by an inverse Fourier transform.[34] Many samples are generated for the given geometrical and roughness parameters, then characteristics of each device is analyzed followed by an ensemble average.[35]

TABLE I. The on-site potentials and hopping parameters of graphene. All values are in the unit of eV.

ε_s	ε_p	$ss\sigma$	$sp\sigma$	$pp\sigma$	$pp\pi$
−7.3	0	−4.30	+4.98	+6.38	−2.66

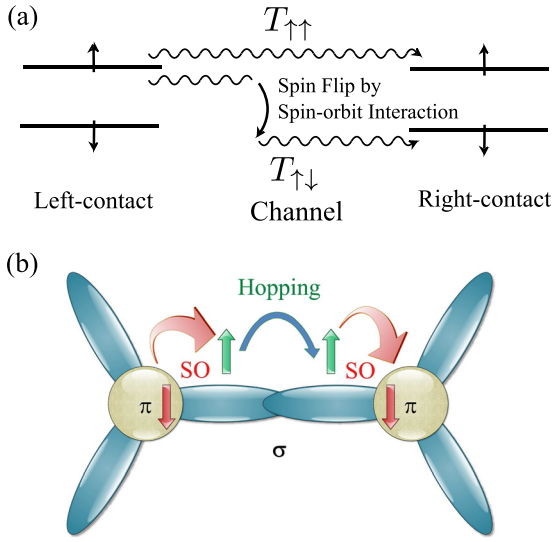

FIG. 1. (a) The illustration of spin transport in a corrugated graphene nanoribbon. (b) Spin transitions due to spin-orbit interaction in $p_{x,y,z}$ orbitals.

The amplitude of the surface roughness depends on the underlying substrate material and the polishing method (see Table II). Surface roughness alters the positions and directions of atomic orbitals of graphene. The hopping parameters have been modulated using Harrison's model $t_{ij} \propto 1/d^2$ (Ref. 36) and the effect of orbital direction variation on the hoping parameters has been included by Slater-Koster model.[37]

The non-equilibrium Green's function (NEGF) is used to study spin transport in corrugated armchair graphene nanoribbons (AGNRs). The Green's function of the channel is given by

$$\begin{pmatrix} G^{r,a}_{\uparrow\uparrow}(\epsilon) & G^{r,a}_{\uparrow\downarrow}(\epsilon) \\ G^{r,a}_{\downarrow\uparrow}(\epsilon) & G^{r,a}_{\downarrow\downarrow}(\epsilon) \end{pmatrix} = \left[(\epsilon \pm i\eta)I - \begin{pmatrix} H_{\uparrow\uparrow} & H_{\uparrow\downarrow} \\ H_{\downarrow\uparrow} & H_{\downarrow\downarrow} \end{pmatrix} - \begin{pmatrix} \Sigma_{L\uparrow} & 0 \\ 0 & \Sigma_{L\downarrow} \end{pmatrix} - \begin{pmatrix} \Sigma_{R\uparrow} & 0 \\ 0 & \Sigma_{R\downarrow} \end{pmatrix}\right]^{-1}, \tag{6}$$

where η is an infinitesimal quantity and $\Sigma_{R/L,\sigma}$ is the self energy of the left or right contact for electrons with up or down spin ($\sigma = \uparrow, \downarrow$) that is given by

$$\Sigma_{\alpha,\sigma} = \tau^{\dagger}_{\alpha,\sigma} g_{\alpha,\sigma}(\epsilon)\tau_{\alpha,\sigma}. \tag{7}$$

g_α is the surface Green's function of semi-infinite left and right electrodes which can be obtained from highly convergent Sancho method.[38] The transmission probability can be obtained by[39]

TABLE II. Surface roughness parameters of some common substrate materials for graphene.[25–27,51–58]

	SiC	SiO_2	BN	Mica	Al_2O_3
δh	10–27 pm	168–360 pm	30–75 pm	24 pm	330 pm
$L_x = L_y$	…	15–32 nm	…	2 nm	…

$$T_{\uparrow\uparrow} = \mathrm{Trace}[\Gamma_{L\uparrow} G^r_{\uparrow\uparrow} \Gamma_{R\uparrow} G^a_{\uparrow\uparrow}], \tag{8a}$$

$$T_{\uparrow\downarrow} = \mathrm{Trace}[\Gamma_{L\uparrow} G^r_{\uparrow\downarrow} \Gamma_{R\downarrow} G^a_{\downarrow\uparrow}], \tag{8b}$$

where $T_{\uparrow\uparrow}$ denotes the transmission probability of carriers with up-spin in the left contact to up-spin in the right-contact and $T_{\uparrow\downarrow}$ refers the transmission probability of carriers with up-spin in the left-contact to down-spin in the right-contact as shown in Fig. 1(a). $T_{\uparrow\downarrow}$ is an indication of spin-flip along the channel due to spin-orbit interaction. Corrugation and spin-orbit interaction are neglected in the contacts. $\Gamma_{\alpha\sigma}$ is the broadening of the left and right-contacts for up- and down-spins, which is defined as

$$\Gamma_{\alpha,\sigma} = i(\Sigma_{\alpha,\sigma}(\epsilon) - \Sigma^{\dagger}_{\alpha,\sigma}(\epsilon)). \tag{9}$$

III. RESULTS AND DISCUSSION

$T_{\uparrow\uparrow}$ and $T_{\uparrow\downarrow}$ for an AGNR are plotted as a function of energy at various roughness amplitudes in Fig. 2. To understand the behavior of transmission probabilities, one should note that surface roughness causes two scattering processes: (I) spin flipping due to enhanced spin-orbit interaction (spin-flip) and (II) scattering due to random variation of hopping parameters. Therefore, both of these mechanisms results in a descending behavior of $T_{\uparrow\uparrow}$ with roughness amplitude. The behavior of $T_{\uparrow\downarrow}$ is more complicated: at small roughness values the latter dominated that enhances spin-flip rate which in turn increases $T_{\uparrow\downarrow}$, while at larger roughness values the former dominates which results in the reduction of $T_{\uparrow\downarrow}$. To focus on spin-flipping process spin-polarization can be defined as[40]

$$P = \frac{T_{\uparrow\uparrow} - T_{\uparrow\downarrow}}{T_{\uparrow\uparrow} + T_{\uparrow\downarrow}}, \tag{10}$$

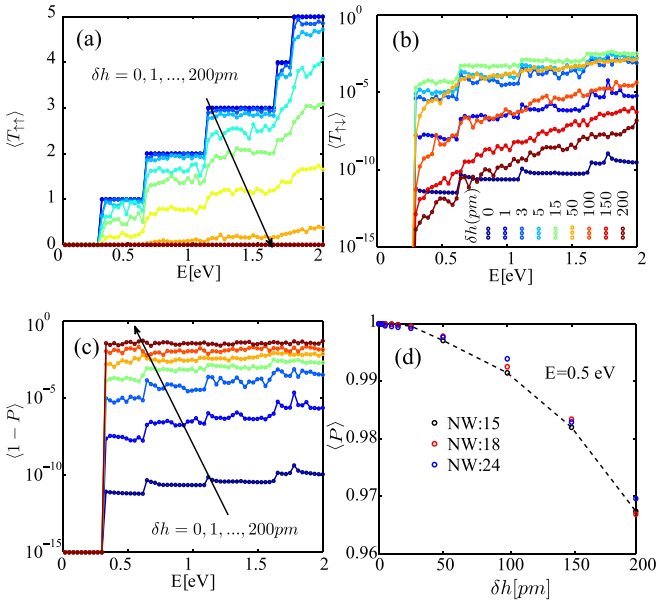

FIG. 2. The ensemble average of (a) $T_{\uparrow\uparrow}$, (b) $T_{\uparrow\downarrow}$, and (c) $1 - P$ as a function of energy at various sub- strate surface roughness amplitudes in AGNR with $nw = 15$, $L = 40$ nm, and $L_x, L_y = 10$ nm and (d) P versus substrate surface roughness amplitude at 0.5 eV with different channel widths. The ribbon index nw denotes the number of dimmer lines across the ribbon width and L is the channel length.

which is a measure of spin-polarization of carriers through the channel, while $1 - \langle P \rangle = 2T_{\uparrow\downarrow}/(T_{\uparrow\uparrow} + T_{\uparrow\downarrow})$ is a measure of spin-flip. As shown in Figs. 2(c) and 2(d), P decreases as roughness amplitude increases. Furthermore, it is clear that the channel width does not have salient effect on the polarization indicating that spin-flip rate enhances as a consequence of surface roughness increase.[2,41,42] The local curvature induced by surface roughness mixes π and σ bonding which enhances spin-flip rate. Thus, the mechanism of spin relaxation of surface roughness is of Elliott-Yafet type.

Correlation length has a different effect on the transmission probability, see Fig. 3. Apparently, $T_{\uparrow\uparrow}$ increases with correlation length, because a longer correlation length leads to a smoother substrate surface which results in the reduction of scattering and spin-flip rate. Therefore, both $T_{\uparrow\uparrow}$ and polarization increase with correlation length.

Spin flipping occurs during carrier transport through the channel. The effects of the channel length on the spin transmission are investigated in Fig. 4. $T_{\uparrow\uparrow}$ decreases as the channel length increases due to increased scattering and spin-flipping rates, while $T_{\uparrow\downarrow}$ shows a more complicated behavior. For short channel lengths transport is nearly ballistic and $T_{\uparrow\downarrow}$ increases with the channel length due to spin-flip increase. In channels longer than the mean free path scattering dominates and consequently $T_{\uparrow\downarrow}$ decreases as the channel length increases (Fig. 4(b)). The polarization versus energy at various channel lengths is shown in Fig. 4. To quantify the effect of surface corrugation on the spin-polarization, one can define spin diffusion length (λ_s) as $P(\epsilon) = P_0 \exp(-L/\lambda_s(\epsilon))$. To extract spin diffusion length, the polarization as a function of channel length is plotted (Fig. 4(c)) and an exponential curve is fitted and the respective λ_s is evaluated. The extracted spin diffusion length for various surface roughness amplitudes and assumed values of the correlation lengths is presented in Table III.

For a surface roughness amplitude of 200 pm, which is a typical value for graphene on SiO_2 substrate, the spin diffusion length is approximately 2.24 μm which is in agreement with experimental values that are reported to be in the range of 1–3 μm at room temperature.[5,6,43–47] The corresponding spin relaxation time can be obtained from $\tau_s = \lambda^2/D_s$. Assuming a spin diffusion coefficient of $D_s \approx 10^{-2}\mathrm{m}^2/\mathrm{s}$,[6] the spin relaxation time will be approximately 500 ps.

For graphene on a boron-nitride substrate with a roughness amplitude of 50 pm, the calculated spin-diffusion length

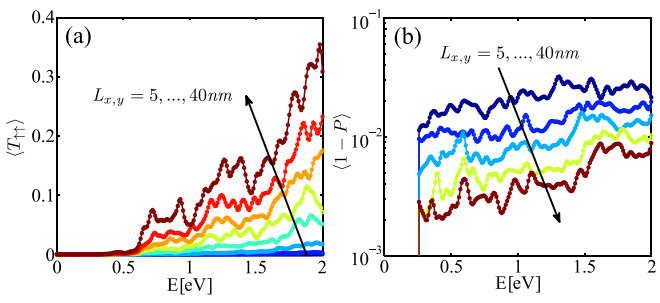

FIG. 3. (a) $T_{\uparrow\uparrow}$ and (b) polarization as a functions of energy at various roughness correlation lengths for AGNR with $nw = 15$, $L = 40$ nm and $\delta h = 100$ pm.

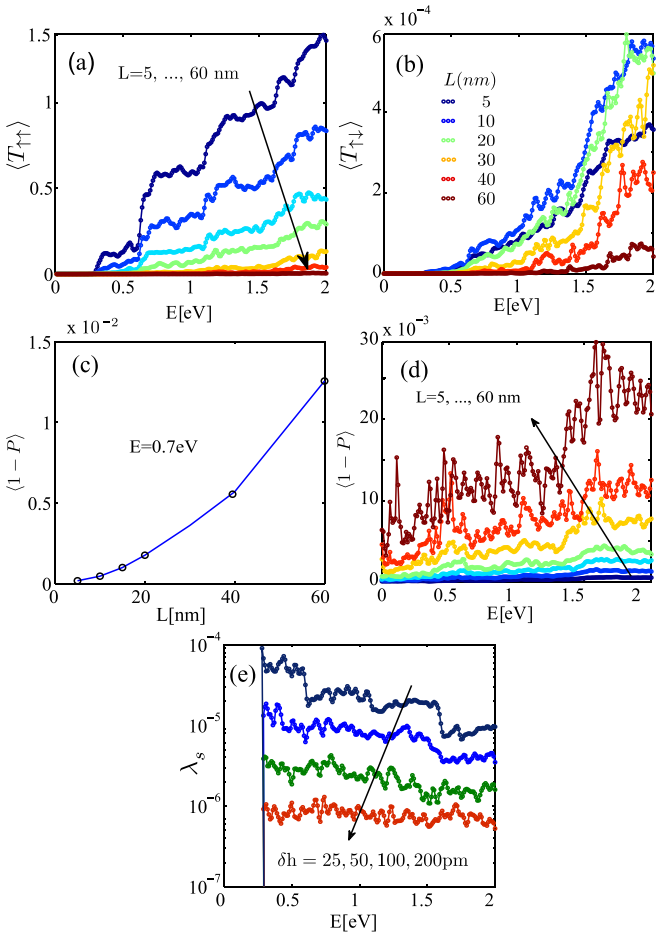

FIG. 4. The ensemble averages of (a) $T_{\uparrow\uparrow}$, (b) $T_{\uparrow\downarrow}$ as functions of energy at various channel lengths, the polarization as a function of (c) channel length, (d) energy for $nw = 15$, $\delta h = 75$ pm and L_x, $L_y = 10$ nm, and (e) spin-diffusion length (λ_s) at various roughness amplitudes.

is 12 μm, which is also in good agreement with experiments that is approximately 10 μm.[15,48] In addition, the spin diffusion length for graphene on SiC substrate with a roughness amplitude of 10 pm is calculated to be 340 μm, which is in good agreement with the experimental value of 285 μm.[7] The small discrepancy between theory and experiments is due to the absence of other spin-relaxation sources in our model. Surface roughens is the dominant spin-relaxation mechanism at large values of roughness amplitude, while at smaller roughness amplitudes other sources should be accounted for.

Experiments prove a weak dependence of spin-diffusion length on temperature[46] implying that charged impurity scattering is not the primary source of spin relaxation[49,50] and the main spin scattering mechanism in graphene is Eliot-Yafet type. This proves our results that surface roughness is the main source of spin relaxation in graphene.

TABLE III. Spin diffusion length for various values of δh.

δh	10 pm	25 pm	50 pm	75 pm	100 pm	150 pm	200 pm
$L_x = L_y$	1 nm	2 nm	5 nm	7 nm	10 nm	15 nm	20 nm
L_s	338 μm	55 μm	12 μm	4.7 μm	3.47 μm	3.27 μm	2.24 μm

IV. CONCLUSIONS

The effects of surface roughness on spin transport in AGNR are investigated, employing the NEGF along with a multi-orbital atomistic tight-binding bandstructure model. It is shown that surface roughness amplitude has a significant influence on spin-polarization. By increasing the roughness amplitude, the spin-polarization decreases due to increased spin-flip rate that is induced by the enhancement of coupling of σ and π orbitals with surface roughness. However, the increase of the correlation length leads to the conservation of spin-polarization over longer channel lengths. Our predicted values of spin-diffusion lengths are close to experimental values. Our finding indicates the importance of including surface roughness for understanding the relatively small spin-relaxation time observed in graphene on substrates.

ACKNOWLEDGMENTS

This work was supported in part by Iran National Science Fund (INSF). The authors gratefully acknowledge the Sheikh Bahaei National High Performance Computing Center (SBNHPCC) for providing computing facilities and time. SBNHPCC was supported by Scientific and Technological Department of Presidential Office and Isfahan University of Technology (IUT).

[1]S. Wolf, D. Awschalom, R. Buhrman, J. Daughton, S. Von Molnar, M. Roukes, A. Y. Chtchelkanova, and D. Treger, Science **294**, 1488 (2001).
[2]D. Huertas-Hernando, F. Guinea, and A. Brataas, Phys. Rev. B **74**, 155426 (2006).
[3]K. S. Novoselov, A. K. Geim, S. Morozov, D. Jiang, Y. Zhang, S. Dubonos, I. Grigorieva, and A. Firsov, Science **306**, 666 (2004).
[4]W. Han, R. K. Kawakami, M. Gmitra, and J. Fabian, Nat. Nanotechnol. **9**, 794 (2014).
[5]N. Tombros, C. Jozsa, M. Popinciuc, H. T. Jonkman, and B. J. Van Wees, Nature **448**, 571 (2007).
[6]W. Han and R. K. Kawakami, Phys. Rev. Lett. **107**, 047207 (2011).
[7]B. Dlubak, M.-B. Martin, C. Deranlot, B. Servet, S. Xavier, R. Mattana, M. Sprinkle, C. Berger, W. A. De Heer, F. Petroff *et al.*, Nat. Phys. **8**, 557 (2012).
[8]D. Pesin and A. H. MacDonald, Nat. Mater. **11**, 409 (2012).
[9]H. Min, J. E. Hill, N. A. Sinitsyn, B. R. Sahu, L. Kleinman, and A. H. MacDonald, Phys. Rev. B **74**, 165310 (2006).
[10]Y. Yao, F. Ye, X.-L. Qi, S.-C. Zhang, and Z. Fang, Phys. Rev. B **75**, 041401 (2007).
[11]M. Gmitra, S. Konschuh, C. Ertler, C. Ambrosch-Draxl, and J. Fabian, Phys. Rev. B **80**, 235431 (2009).
[12]J. C. Boettger and S. B. Trickey, Phys. Rev. B **75**, 121402 (2007).
[13]C. L. Kane and E. J. Mele, Phys. Rev. Lett. **95**, 226801 (2005).
[14]C. Ertler, S. Konschuh, M. Gmitra, and J. Fabian, Phys. Rev. B **80**, 041405 (2009).
[15]M. Drögeler, F. Volmer, M. Wolter, B. Terrés, K. Watanabe, T. Taniguchi, G. Guntherodt, C. Stampfer, and B. Beschoten, Nano Lett. **14**, 6050 (2014).
[16]M. H. D. Guimarães, P. J. Zomer, J. Ingla-Aynés, J. C. Brant, N. Tombros, and B. J. Van Wees, Phys. Rev. Lett. **113**, 086602 (2014).
[17]S. Roche and S. O. Valenzuela, J. Phys. D: Appl. Phys. **47**, 094011 (2014).
[18]S. Roche, B. Beschoten, J.-C. Charlier, M. Chshiev, S. P. Dash, B. Dlubak, J. Fabian, A. Fert, F. Guinea, I. Grigorieva *et al.*, 2D Mater. **2**, 030202 (2015).
[19]A. Varykhalov, J. Sánchez-Barriga, A. M. Shikin, C. Biswas, E. Vescovo, A. Rybkin, D. Marchenko, and O. Rader, Phys. Rev. Lett. **101**, 157601 (2008).
[20]M. Gmitra, D. Kochan, and J. Fabian, Phys. Rev. Lett. **110**, 246602 (2013).

[21]D. Kochan, M. Gmitra, and J. Fabian, Phys. Rev. Lett. **112**, 116602 (2014).
[22]D. Huertas-Hernando, F. Guinea, and A. Brataas, Phys. Rev. Lett. **103**, 146801 (2009).
[23]A. H. CastroNeto and F. Guinea, Phys. Rev. Lett. **103**, 026804 (2009).
[24]K. Pi, W. Han, K. McCreary, A. Swartz, Y. Li, and R. Kawakami, Phys. Rev. Lett. **104**, 187201 (2010).
[25]M. Ishigami, J. H. Chen, W. G. Cullen, M. S. Fuhrer, and E. D. Williams, Nano Lett. **7**, 1643 (2007).
[26]C. H. Lui, L. Liu, K. F. Mak, G. W. Flynn, and T. F. Heinz, Nature **462**, 339 (2009).
[27]V. Geringer, M. Liebmann, T. Echtermeyer, S. Runte, M. Schmidt, R. Rückamp, M. C. Lemme, and M. Morgenstern, Phys. Rev. Lett. **102**, 076102 (2009).
[28]D. Gosálbez-Martínez, J. J. Palacios, and J. Fernández-Rossier, Phys. Rev. B **83**, 115436 (2011).
[29]D. Huertas-Hernando, F. Guinea, and A. Brataas, Eur. Phys. J.: Spec. Top. **148**, 177 (2007).
[30]V. K. Dugaev, E. Y. Sherman, and J. Barnaś, Phys. Rev. B **83**, 085306 (2011).
[31]M. Pourfath, *The Non-Equilibrium Green's Function Method for Nanoscale Device Simulation* (Springer, 2014).
[32]J. Serrano, M. Cardona, and T. Ruf, Solid-State Commun. **113**, 411 (2000).
[33]F. Herman and S. Skillman, *Atomic Structure Calculations* (Prentice-Hall, 1963).
[34]S. B. Touski and M. Pourfath, Appl. Phys. Lett. **103**, 143506 (2013).
[35]A. Yazdanpanah, M. Pourfath, M. Fathipour, H. Kosina, and S. Selberherr, IEEE Trans. Electron Devices **59**, 433 (2012).
[36]W. A. Harrison, *Elementary Electronic Structure* (World Scientific, 1999).
[37]D. Papaconstantopoulos and M. Mehl, J. Phys.: Condens. Matter **15**, R413 (2003).
[38]M. L. Sancho, J. L. Sancho, and J. Rubio, J. Phys. F: Met. Phys. **14**, 1205 (1984).
[39]B. Wang, J. Wang, and H. Guo, J. Phys. Soc. Jpn. **70**, 2645 (2001).
[40]V. I. Perel', S. A. Tarasenko, I. N. Yassievich, S. D. Ganichev, V. V. Bel'kov, and W. Prettl, Phys. Rev. B **67**, 201304 (2003).
[41]L. Chico, M. P. López-Sancho, and M. C. Muñoz, Phys. Rev. B **79**, 235423 (2009).
[42]M. P. López-Sancho and M. C. Munoz, Phys. Rev. B **83**, 075406 (2011).
[43]W. Han, K. Pi, W. Bao, K. McCreary, Y. Li, W. Wang, C. Lau, and R. Kawakami, Appl. Phys. Lett. **94**, 222109 (2009).
[44]M. Popinciuc, C. Józsa, P. J. Zomer, N. Tombros, A. Veligura, H. T. Jonkman, and B. J. Van Wees, Phys. Rev. B **80**, 214427 (2009).
[45]Y. Liu, H. Idzuchi, Y. Fukuma, O. Rousseau, Y. Otani, and W. Lew, Appl. Phys. Lett. **102**, 033105 (2013).
[46]A. Avsar, T.-Y. Yang, S. Bae, J. Balakrishnan, F. Volmer, M. Jaiswal, Z. Yi, S. R. Ali, G. Guntherodt, B. H. Hong *et al.*, Nano Lett. **11**, 2363 (2011).
[47]M. H. D. Guimãraes, A. Veligura, P. J. Zomer, T. Maassen, I. J. Vera-Marun, N. Tombros, and B. van Wees, Nano Lett. **12**, 3512 (2012).
[48]W. Fu, P. Makk, R. Maurand, M. Bräuninger, and C. Schönenberger, J. Appl. Phys. **116**, 074306 (2014).
[49]W. Han, K. McCreary, K. Pi, W. Wang, Y. Li, H. Wen, J. Chen, and R. Kawakami, J. Magn. Magn. Mater. **324**, 369 (2012).
[50]W. Han, J.-R. Chen, D. Wang, K. M. McCreary, H. Wen, A. G. Swartz, J. Shi, and R. K. Kawakami, Nano Lett. **12**, 3443 (2012).
[51]C. R. Dean, A. F. Young, I. Meric, C. Lee, L. Wang, S. Sorgenfrei, K. Watanabe, T. Taniguchi, P. Kim, K. Shepard *et al.*, Nat. Nanotechnol. **5**, 722 (2010).
[52]S.-Y. Kwon, C. V. Ciobanu, V. Petrova, V. B. Shenoy, J. Bareno, V. Gambin, I. Petrov, and S. Kodambaka, Nano Lett. **9**, 3985 (2009).
[53]X. Wang, S. M. Tabakman, and H. Dai, J. Am. Chem. Soc. **130**, 8152 (2008).
[54]J. Xue, J. Sanchez-Yamagishi, D. Bulmash, P. Jacquod, A. Deshpande, K. Watanabe, T. Taniguchi, P. Jarillo-Herrero, and B. J. LeRoy, Nat. Mater. **10**, 282 (2011).
[55]A. Zugarramurdi, M. Debiossac, P. Lunca-Popa, A. Mayne, A. Momeni, A. Borisov, Z. Mu, P. Roncin, and H. Khemliche, Appl. Phys. Lett. **106**, 101902 (2015).
[56]S. Berner, M. Corso, R. Widmer, O. Groening, R. Laskowski, P. Blaha, K. Schwarz, A. Goriachko, H. Over, S. Gsell *et al.*, Angew. Chem., Int. Ed. **46**, 5115 (2007).
[57]P. Lauffer, K. V. Emtsev, R. Graupner, T. Seyller, L. Ley, S. A. Reshanov, and H. B. Weber, Phys. Rev. B **77**, 155426 (2008).
[58]V. W. Brar, Y. Zhang, Y. Yayon, T. Ohta, J. L. McChesney, A. Bostwick, E. Rotenberg, K. Horn, and M. F. Crommie, Appl. Phys. Lett. **91**, 122102 (2007).